Clim Dyn
DOI 10.1007/s00382-015-2564-7

A conceptual model for glacial cycles and the middle Pleistocene transition

István Daruka[1] · **Peter D. Ditlevsen**[2]

Received: 5 August 2014 / Accepted: 16 March 2015

Abstract Milankovitch's astronomical theory of glacial cycles, attributing ice age climate oscillations to orbital changes in Northern-Hemisphere insolation, is challenged by the paleoclimatic record. The climatic response to the variations in insolation is far from trivial. In general the glacial cycles are highly asymmetric in time, with slow cooling from the interglacials to the glacials (inceptions) and very rapid warming from the glacials to the interglacials (terminations). We shall refer to this fast-slow dynamics as the "saw-tooth" shape of the paleoclimatic record. This is non-linearly related to the time-symmetric variations in the orbital forcing. However, the most pronounced challenge to the Milankovitch theory is the middle Pleistocene transition (MPT) occurring about one million years ago. During that event, the prevailing 41 kyr glacial cycles, corresponding to the almost harmonic obliquity cycle were replaced by longer saw-tooth shaped cycles with a timescale around 100 kyr. The MPT must have been driven by internal changes in climate response, since it does not correspond to any apparent changes in the orbital forcing. In order to identify possible mechanisms causing the observed changes in glacial dynamics, it is relevant to study simplified models with the capability of generating temporal behavior similar to the observed records. We present a simple oscillator type model approach, with two variables, a temperature anomaly and a climatic memory term. The generalization of the ice albedo feedback is included in terms of an effective multiplicative coupling between this latter climatic memory term (representing the internal degrees of freedom) and the external drive. The simple model reproduces the temporal asymmetry of the late Pleistocene glacial cycles and suggests that the MPT can be explained as a regime shift, aided by climatic noise, from a period 1 frequency locking to the obliquity cycle to a period 2–3 frequency locking to the same obliquity cycle. The change in dynamics has been suggested to be a result of a slow gradual decrease in atmospheric greenhouse gas concentration. The critical dependence on initial conditions in the (non-autonomous) glacial dynamics raises fundamental questions about climate predictability.

Keywords Milankovitch theory · Glacial cycles · Mid-Pleisocene transition

1 Introduction

The Pleistocene climate evolution is documented in the global stacked marine core benthic foraminiferal $\delta^{18}O$ record (Shackleton 1997; Lisiecki and Raymo 2005). This is a combined proxy for global ice volume and ocean temperature. The stacked record correlates strongly with the Antarctic ice core isotope records (Petit 2001; Augustin et al. 2004) for the past 420 and 800 kyr, which thus in this context provides limited additional information. It should, however, be noted that leads and lags between the different records and lags to the insolation obviously carry essential climatic information, but at present the accuracy of the uncertainty in the dating of the marine cores is of the order

✉ Peter D. Ditlevsen
pditlev@nbi.ku.dk

István Daruka
Istvan.Daruka@jku.at

[1] Institute of Semiconductor and Solid State Physics, Johannes Kepler University, Altenbergerstrasse 69, 4040 Linz, Austria

[2] Centre for Ice and Climate, Niels Bohr Institute, University of Copenhagen, Juliane Maries Vej 30, 2100 Copenhagen O, Denmark

Published online: 31 March 2015

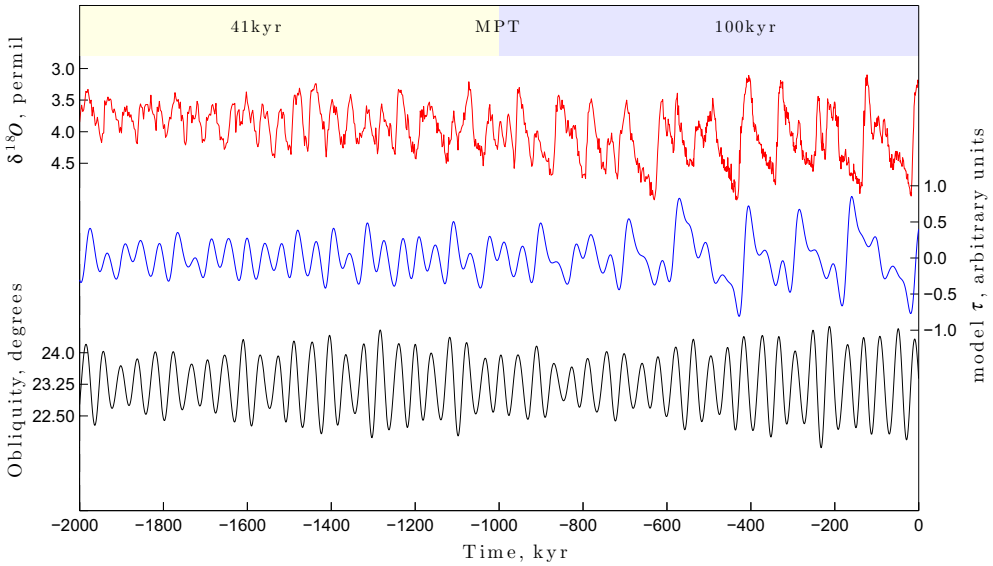

Fig. 1 The middle Pleistocene transition (MPT). The *red curve* corresponds to the composite deep sea foraminiferal isotope record (Lisiecki and Raymo 2005). The MPT is seen as a change around 1 Myr BP in period from 41 kyr in the early Pleistocene to approximately 100 kyr in the late Pleistocene. The former cycles are symmetric, while the latter cycles are asymmetric ('saw-tooth shaped'). The *blue curve* shows the model results for the related temperature anomaly when driven by real obliquity data (Berger and Loutre 1991), represented by the *black curve*. The parameter values used for this plot are discussed in the text

millennia, which makes it difficult to establish detailed causal relations between the different proxies. The limited knowledge of regional climate variations across glacial cycles and the apparent synchronization of the global climate response to the Milankovitch forcing, makes it potentially impossible to discriminate between possible physical mechanisms for explaining the dynamics. This is simply because of the presence of synchronization with the forcing in the models (Tziperman et al. 2006).

Since the climate response to insolation changes is strongly influenced by the summer melt of the ice sheets, the 65N summer solstice insolation is most often identified as the "Milankovitch forcing" (Berger 1988, 2012). However, this particular component of the insolation is most strongly influenced by the approximately 20 kyr precessional cycle, whereas the paleoclimatic record shows that the response is strongest in the 41 and 100 kyr bands. The glacial melt depends rather on the integrated summer insolation (as an indicator of positive degree days) than on the summer solstice insolation. The integrated summer insolation is indeed dominated by the 41 kyr obliquity cycle (Huybers 2006). This compares well with the climate record prior to the middle Pleistocene transition (MPT) 41 kyr world, while the late Pleistocene 100 kyr world compares more with the variations in the eccentricity of the orbit. The changes in insolation due to changes in eccentricity are an order of magnitude smaller than the changes due to the change in obliquity. The effect of the change in eccentricity is mainly through the amplification of the precessional cycle; when eccentricity is high the effect of precession is high, and when the eccentricity is small, the effect of precession (distance to the Sun as a function of season) vanishes. The lack of spectral power in the 100 kyr band in insolation is referred to as the 100 kyr problem of the Milankovich theory (Imbrie et al. 1993; Hays et al. 1976). The solution to this problem is probably that the 100 kyr world is not paced by eccentricity, which is also why the 400 kyr modulation to the eccentricity is not seen in the climatic response. This is referred to as the 400 kyr problem or the Stage 11 problem: Marine isotope stage 11 (MIS-11) should not have been an interglacial if changes in eccentricity were the driver. It has been suggested that the 100 kyr world could rather be seen as multiplets of the 41 kyr obliquity cycle, such that they are approximately 80 and 120 kyr long, occurring in a more or less alternating way (Huybers 2007; Ditlevsen 2009). Note in Fig. 1 that the duration between the warm states around 200 kyr BP (MIS-7 and MIS-6) is approximately 40 kyr.

Since there are no apparent changes in the astronomical forcing at the MPT, the transition must be governed by the internal dynamical response to the forcing. The hypothesis is that a gradual change in some environmental parameter of the system led to a dynamical change in the response to the orbital forcing. Two main hypotheses have been put forward for the change in environment; either a slow decrease in atmospheric pCO_2 (Saltzman and Maasch 1991) led to

reduced greenhouse warming and the possibility of deeper glaciations, or slow glacial erosion of the regolith under the glaciers, such that the glaciers after the MPT would grow on the bedrock, which permits higher glaciers to be stable (Clark and Pollard 1998). For a review see Clark et al. (2006). Here we shall argue by introducing a conceptual climate oscillator model that the MPT could be a result of frequency locking to the orbital forcing in such a way that a slight change in parameters can change the period of the frequency locking.

The phenomenon of frequency locking for explaining climatic response to orbital forcing has been suggested before. De Saedeleer et al. discuss in terms of the Van der Pol oscillator the possibility of synchronizing to spectral components of the 65N summer solstice insolation (Saedeleer et al. 2013). These are expressed in terms of a trigonometric series resulting from the perturbative calculation of the orbital parameters (Berger 1978). Further aspect in synchronization are the relative phases (Crucifix 2013) and the pullback attractor for a given synchronization (Chekroun et al. 2011).

Here we are not so much concerned with the problem of which components of the orbital forcing the climate system is most sensitive to. Since the different orbital parameters influence the insolation very differently in both seasonality and in latitudinal variation it is unlikely that a single time series (such as the 65N summer solstice insolation) is sufficient to give the full account of the Pleistocene glacial cycles.

It is still an open problem to which extent the global stack marine isotope record itself is sufficient to discriminate between the suggested low dimensional or conceptual models of the Pleistocene glacial cycles. A decisive model of the MPT probably have to wait for future comprehensive climate model simulations and strong improvements in the regional climate reconstructions. Exploring alternative mechanisms in simple and conceptual models are thus important both for identifying robust features and for discriminating through hypothesis testing.

2 Existing models

In order to put our model into perspective, in the following we summarize some of the proposed models and their limitations. This is by no means a comprehensive review. The models of glacial cycles can roughly be categorized in two types: First, mono- or multi-stable state models where the periodicity is solely a result of the periodicity of the orbital forcing. Secondly, climate oscillator models where the glacial cycles in one way or another result from the internal oscillator resonating with the orbital forcing. For a thorough review of oscillator type models see Crucifix (2012).

The classical energy balance models (Budyko 1969; Sellers 1969) belong to the first category. In these models the ice-albedo feedback results in a two-state system, a present climate state and a glaciated state, which today is considered more realistically to describe the Snowball Earth climate. The relative weakness in the magnitude of the 100 kyr eccentricity cycle in insolation led to the introduction of the concept of stochastic resonance (Benzi et al. 1982).

For contrasting the glacial dynamics before and after the MPT a semi-empirical model was proposed by Paillard (1998). The model is a rule based threshold model with three possible stable climate states, an interglacial, a mild glacial and a full glacial. With specific rules of transitions and a slow change of threshold, the model reproduces the Pleistocene record including the MPT as a response to the Milankovitch forcing. An empirical dynamical model, with a three stable state bifurcation diagram, explaining the specific rules of transitions in the Paillard model has been proposed (Ditlevsen 2009). In this model a change of the bifurcation structure causes the MPT. A different approach was taken in Huybers and Wunsch (2005) for explaining the 100 kyr world as a result of the 41 kyr orbital forcing. This is a stochastic threshold model with a linear drift towards glaciation. When a threshold proportional to the obliquity forcing is reached the glaciation terminates and the climate is reset to the interglacial condition. This model naturally reproduces the saw-tooth shape of the climate curve. The linear drift assumes a very long internal time-scale of the order 100 kyr for glaciation. By a simple rescaling the model can also reproduce the 41 kyr world, however, with more time asymmetric (saw-tooth shaped) glaciations, than observations indicate.

Many different types of oscillator models have been suggested: The dynamics of ice sheets is roughly : Higher temperature $\rightarrow$ higher accumulation $\rightarrow$ growing ice sheet $\rightarrow$ high albedo $\rightarrow$ lower temperature (Kallen et al. 1979; Tziperman and Gildor 2003). This results in free oscillations of the order 5–15 kyr, which are too fast to account for the glacial cycles. The non-linear response in this model to beat periods (combination tones) between the 19 and 23 kyr precessional frequencies has been suggested to explain the 100 kyr glacial cycles (LeTreut and Ghil 1983). To obtain free climate oscillations of as long a duration as 100 kyr, the combined effect of isostatic rebound and reduced accumulation with a high ice sheet (the elevation desert effect) is another suggestion (Hyde and Peltier 1985). None of these models attempt to explain the MPT shift in glacial periods. It was suggested by Salzman and Maasch (1991) that the ice sheet growth is controlled by the deep ocean temperature: low ocean temperature $\rightarrow$ higher uptake of atmospheric $\rightarrow$ less greenhouse warming $\rightarrow$ growth of ice sheets and sea ice $\rightarrow$ reduced meridional oceanic heat transport $\rightarrow$ higher ocean temperature. In

the model this is a limit cycle, which is initiated at the MPT through a Hopf bifurcation as a result of a slow decrease in pCO_2 from increased weathering. This model is not concerned with the 41 kyr climate oscillations prior to the MPT. A switch mechanism involving the sea ice was proposed by Tziperman and Gildor (2003). In this model the feedback loop is: High sea ice cover (limited by the warm mid-latitude ocean) → reduced atmospheric temperature and precipitation (accumulation) over the ice sheets → negative mass balance → rapid retreat of the ice sheets → reduced albedo → increased temperature → rapid retreat of the sea ice → increased precipitation and a positive mass balance. This is a relaxation oscillator, where the 100 kyr cycle is internally driven and independent of the orbital forcing. The time-scale for growth of the ice sheets estimated as V/Acc, where V is the volume of the ice sheet and Acc is the accumulation (in suitable units) is of the order 10–30 kyr. The time-scale of 100 kyr glacial cycles in the Tziperman–Gildor model is rather estimated from $V/Acc–Abl$, where $(Acc–Abl)$ is the difference between accumulation and ablation in the growth phase. In principle this estimate is not well constrained, since in the case of almost mass balance this growing time is infinite. If the deep ocean in the model is warm enough, the sea-ice-switch is not active, and the model oscillates linearly with the orbital forcing. The gradual cooling of the deep ocean, crossing a threshold at MPT activates the sea-ice-switch mechanism and the 100 kyr oscillations of the late Pleistocene period. Alternatively, the 41 kyr world could be self-sustained oscillations, perhaps locked to the obliquity cycles (Ashkenazy and Tziperman 2004). Yet another conceptual relaxation oscillator model (Paillard and Parrenin 2004) has been proposed, pointing to the mechanism of atmospheric pCO_2 being governed by the slow ventilation of the deep ocean, which in turn is governed by the salination of the deep ocean from sea ice brine rejection and deposition of freshwater in the ice sheets. In this model the atmospheric pCO_2 is governed by a threshold function of the ocean ventilation, which by introducing a slow millennial scale drift in the ventilation can reproduce the MPT as a response to the 65N summer solstice insolation.

All the above suggested physical mechanisms are potentially at play in the climate system, thus it is difficult to assess the relative importance without realistic quantitative modelling, which at present is computationally prohibited. Conceptual models are useful to identify dynamical mechanisms relevant to explain and predict the evolution of the climate system. Rial (2004) suggested a logistic-delayed differential equation for the ice volume coupled, through a carrying capacity, to a temperature. The temperature is determined by the energy balance between incoming and outgoing radiation. By changing the coupling via the carrying capacity, the MPT is reproduced. The underlying physical mechanism is difficult to identify, partly because delay-equations are notoriously difficult to analyse. An even simpler approach was taken by Huybers (2009), in which the Pleistocene climate is described by a discrete map, where the ice volume depends on the ice volume with a lag of 9 kyr, which is approximately the lag between climate oscillations and their derivative in a 41 kyr harmonic cycle. The hypothesis is that the late Pleistocene cycles are purely chaotic, while the 41 kyr cycles prior to the MPT are results of coincidental oscillations near an unstable period 2 cycle in the map. However, within the model framework, the observed long sequence of 41 kyr cycles prior to the MPT seems highly unlikely.

The conceptual modelling is also our approach here, where we shall argue that the MPT could be a change in the internal dynamics leading to a change in frequency locking to the obliquity cycle. This would imply a fundamental limitation in climate predictability, such as inferences about the next inception. We do, however, find this type of unfalsifiable very long time predictions into the future rather academic, but the suggested critical dependence on model parameters is potentially an important guideline for more realistic future model simulations and theories of the Pleistocene glacial dynamics.

3 Model

The climate system is obviously of very high dimensionality, with dynamics governed by a multitude of processes operating on many different time-scales. The reason that a low dimensional representation can be relevant relies on the assumption that the astronomical forcing is decisive in the dynamics. The astronomical forcing is indeed of low dimensionality governed by only three parameters: precession, obliquity and eccentricity. A second motivation for the conceptual modeling approach is the observation that the (stacked) benthic foraminifera isotope record from ocean sediment cores seems to be a robust climatic signal more-or-less reproduced in all paleoclimatic proxies, indicating a synchronous global climate response to the orbital forcing. In the following we shall refer to this record simply as the "climate record".

As a minimal modeling approach we explore a two variable non-linear oscillator model. The first variable τ is targeting the climate record. This proxy reflects both the global ice volume, through the increase in heavy isotope water concentration in the ocean when ice masses built up, and the deep ocean temperature, through temperature dependent fractionation in foraminiferal growth. Thus τ can be thought of as a global temperature anomaly, proportional to (minus) the global ice volume. The other variable x represents an (unobserved) variable, which determines

the state of the climate and thus holds the long term memory, such as total heat content in the deep ocean. This aligns with the approach of Saltzman and Maasch (1991) and that of Tziperman and Gildor (2003) arguing that besides the ice volume, also the deep sea temperature and possible other factors play a decisive role in determining the internal climate dynamics.

In the light of the above, we consider a simple integrative relation between the effective climatic memory term x and temperature anomaly τ;

$$\dot{x}(t) = \lambda\tau(t), \tag{1}$$

where λ^{-1} represents the time-scale unit of the climatic memory. The paleoclimatic record indicates that the climate can be in one of more possible stable states (Imbrie et al. 2011). Within a two variable model, not resolving this multi-state dynamics, the evolution of the temperature anomaly is represented by an effective climate potential $V(x)$ which could possess different local minima and a damping of the anomaly $(-\kappa\tau)$. The interaction between the internal dynamics and the external drive is modeled as a multiplicative coupling between the solar insolation $A(t)$ and the climatic memory term $x(t)$. Such a multiplicative coupling might correspond to climatic state dependent albedo effects (Kallen et al. 1979). Thus, the evolution equation for the temperature anomaly τ becomes

$$\dot{\tau}(t) = -V'(x(t)) - \kappa\tau(t) - x(t)A(t) + \sigma\eta(t), \tag{2}$$

where $'$ denotes derivative with respect to the argument. The last term is a climatic noise term to account for unresolved processes, where $\eta(t)$ represents a white noise contribution with $\langle\eta(t)\eta(t')\rangle = \delta(t-t')$. Furthermore, we define

$$V(x) = \alpha x - x^2/2 + x^4/4 \tag{3}$$

as the effective climate potential. This is the simplest nontrivial polynomial multiple state potential, which can contain two minima representing two distinct stable climate states. We note that the non-symmetric, non-harmonic nature of the implemented climate potential renders no characteristic time-scale to the climatic response. Note that this potential is not the potential derived from the classical Budyko–Sellers energy balance model (Budyko 1969), now believed to describe the Snowball Earth dynamics (Hoffman et al. 1998).

The model described by Eqs. (1)–(3) is a forced non-linear oscillator, including a multiplicative coupling between the internal dynamics (climatic memory effects) and the external forcing. Note that by differentiating Eq. (3), substituting $x(t) = \lambda\int^t \tau(t')dt'$, we obtain a single second order integro-differential equation for the observable τ alone.

For $\alpha < 2\sqrt{3}/9$, the effective climatic potential (3) has two stable states. Here we shall, however, not be concerned with this strongly non-linear regime. Throughout the rest of the paper we shall use $\alpha = 0.8$ in Eq. (3), thus $V(x)$ is a non-harmonic skewed potential with a single minimum. The major effect of the non-harmonic nature of the potential is that the frequency of free oscillations (in case of no damping and no forcing) depends on the amplitude of oscillation. Thus the system does not have a natural internal frequency of oscillation.

The external drive has a period (time-scale) $T_{ext} = 2\pi/\omega$, where ω is the dominant frequency of the orbital forcing. In this work we shall not so much be concerned with the multi-frequency nature of the orbital forcing (Saedeleer et al. 2013). The orbital changes in insolation strongly depend on latitude and season, which is not directly incorporated in an effective low dimensional model as presented here.

In the following we demonstrate that the model is capable of reproducing the climate record including the MPT and the time asymmetry, the saw-tooth shapes, of the glacial cycles in the 100 kyr world solely as a response to the obliquity cycles. In order to explore the dynamical features of the model, we shall first simplify by applying a pure sinusoidal forcing $A(t) = A\sin(\omega t)$ with a period of 41 kyr, which quite accurately represents the obliquity cycle.

The simple model exhibits surprisingly complex dynamics. Our suggestion is that the MPT is a result of a slow environmental change represented as a slow change in a model parameter. Here we restrict ourselves to changes in the climatic damping coefficient κ. This change results in a shift from a period 1 frequency locking to a period 2 and 3 frequency locking. Such a change in the dynamical response to the forcing results in a very long non-periodic transient response, which might explain why the timing of the MPT is rather unconstrained, varying from 1.2 Myr to 800 kyr.

4 Basic properties of the model

In spite of the apparent simplicity of this conceptual model, it contains a rich dynamics both in its basic mathematical and physical aspects. To illustrate this, we first apply a simple deterministic ($\sigma = 0$) sinusoidal external driving; $A(t) = A\sin(\omega t)$, taking $\omega = 2\pi(41\text{ kyr})^{-1}$ (=15.331 in our units of 100 kyr^{-1}) corresponding to the obliquity cycle. With this choice, the free parameters of the model are: α, A, κ and λ. Again, we use the value $\alpha = 0.8$, corresponding to a climatic potential (V) with a single minimum. Also, if not stated otherwise, we set the parameter $\lambda = 10$ (in appropriate units of 100 kyr^{-1}) throughout our investigations, corresponding to a characteristic time-scale of 10 kyr. The Eqs. (1)–(3) were numerically integrated using a fourth-order Runge–Kutta scheme. As initial conditions,

$\tau_0 = 0$ and $x_0 = -1.2756$ were chosen. The latter value corresponds to the minimum of the climatic potential for $\alpha = 0.8$.

We found the following types of temperature anomaly oscillations: linear response, the response frequency coincides with that of the driving; period doubling, period multiplication, with related "exotic" shaped oscillations; and chaotic behavior.

The period multiplication scenario is shown in Fig. 2 for a section of the (A–κ) parameter space. A standard procedure for identifying periodicity as multiple of the driving period, would be generating a Poincare—or a stroboscopic map, and counting the number of intersections, regarding points within circles of some small radius ϵ as identical. Here we apply a slightly more robust method where the periodicity n is calculated as

$$n = \min_m : \int_{T_{end}-mT}^{T_{end}} |x(t) - x(t - mT)|dt < \epsilon.$$

Figure 2 demonstrates the occurrence of many different multiple periods. Going from right to left in the top panel through periods 1 (white)—2 (yellow)—4 (red), a period doubling route to chaos is observed. The sharp phase boundary lines separating different period oscillations are lines of bifurcation points. Beside the period-doubling bifurcation, there exists other types of bifurcations, such as a period 3 (green) to period 4 (red) close to the first blue mark in Fig. 2 top panel. The full analysis and characterization of the different types of bifurcations is beyond the scope of this paper. Here we remark that a small change in the model parameters can lead to a remarkable transition in the climatic response. As an example, Fig. 3 demonstrates a period doubling transition in the climatic response τ. In the top panel, this bifurcation is triggered by noise, while in the lower panel the bifurcation point is crossed by a very small, gradual change in the sinusoidal drive, which we otherwise consider constant in this paper. In both cases, the response to a slight change in the forcing results not only in a change in periodicity, but also in a change in the amplitude of the response.

In general, we found that the appearance of chaos was promoted at small values of ω, large values of A, large values of λ, and small values of κ. The parameter κ has a dimension of 1/time, thus can be interpreted as an (inverse) time-scale for a Newtonian relaxation back to the mean climatic state. Figure 4 shows the Lyapunov-exponent for the temperature anomaly (defined as $\partial \ln(\delta\tau)/\partial t$) for a section of the ($\lambda$–$\kappa$) phase space where the critical dependence on initial conditions occurs. Interestingly, while in certain directions the Lyapunov exponent changes continuously from zero to a positive value, in other directions one observes an abrupt change. This is

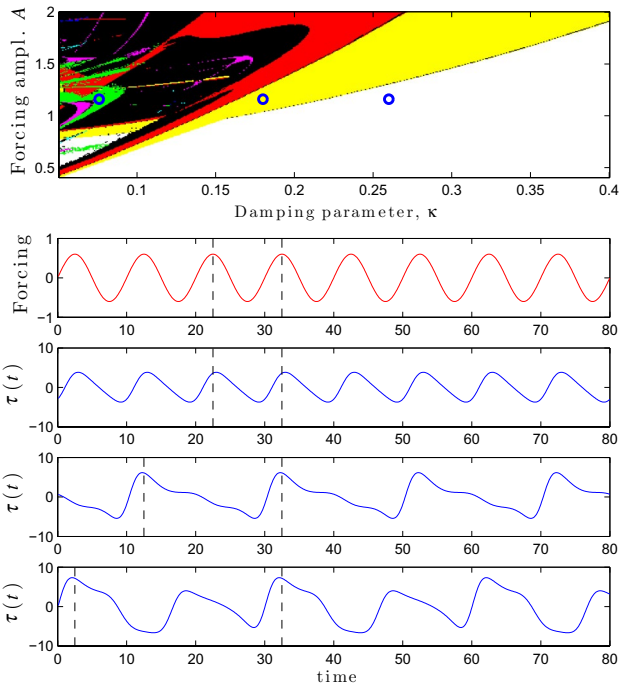

Fig. 2 The behavior of the model driven by a sinusoidal forcing $A\sin(\omega t)$, shown in *red* in the *second panel*. The *top panel* shows the periods in multiplets of the driving period ($2\pi/\omega$): *White* corresponds to periodic solutions with period 1, *yellow* period 2, *green* period 3, *red* period 4, *magenta* period 6, *black* ≥ 8, including non-periodic (chaotic) solutions. The *bottom three panels* show the model temperature anomaly τ corresponding to the *blue circles* in the *top panel right-to-left* (periods 1, 2, 3 as indicated by the *vertical dashed lines*). Changing parameters along a *horizontal line* shows a period doubling route to chaos. We used the parameters $\omega = 2\pi/10$, $\lambda = 0.1$, with $x_0 = 0$, and $\tau_0 = 1$ as initial conditions for this plot

found by numerical investigation, a thorough mathematical treatment is worth pursuing, but well beyond the scope of this paper.

The non-linearity in the model occurs in two terms, the non-harmonic potential and the multiplicative forcing. In the noise free case with the multiplicative forcing substituted by a constant amplitude harmonic forcing, the model reduces in the symmetric case $\alpha = 0$ to the Duffing oscillator: $\ddot{x} = x - x^3 - \kappa\dot{x} + A\sin(\omega t)$. In this case the natural frequency of the system depends on the amplitude of oscillations, which makes the response to the external forcing a resonance phenomenon. In case of multiplicative forcing but with a harmonic potential, we can think of the dynamics as oscillations in a time varying potential $\ddot{x} = (-\omega_0^2 + A\sin(\omega t))x - \kappa\dot{x}$. In the case $\omega_0 \gg \omega$, the potential is quasi-stationary, and the system oscillates with a time varying frequency $\sqrt{\omega_0^2 - A\sin(\omega t)}$. In the case $\omega_0 \ll \omega$ the system will experience a time-mean harmonic potential, and an unaltered natural frequency $\sqrt{\omega_0^2 - \langle A\sin(\omega t)\rangle} = \omega_0$. The case $\omega_0 \approx \omega$,

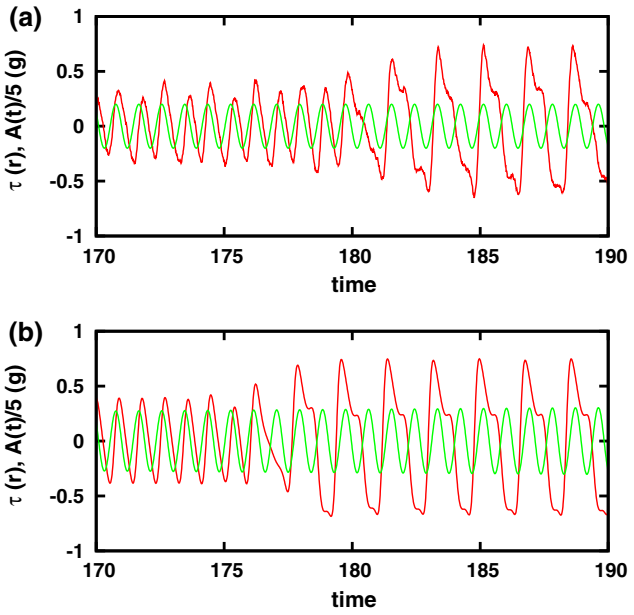

Fig. 3 The model has a period doubling route to chaos. Here we demonstrate the first (pitchfork) bifurcation. **a** The period doubling is induced by additive noise, using a noise amplitude $\sigma = 0.316$ and a climatic drive $A(t) = \sin(\omega t)$. In **b** a very small, visually unnoticeable gradual change in the sinusoidal driving (implementing $A(t) = 0.002t \sin(\omega t)$; plotted in *green*) can lead to the sharp, period doubling in the climatic response τ (plotted in *red*). The remaining parameters we used for these plots are $\omega = 7$, $\lambda = 10$, $\kappa = 1.3$, with $x_0 = -1.2756$, and $\tau_0 = 0$ as initial conditions

which is relevant for this study is much harder to analyse. By numerical investigation, we see that the model combining both types of non-linearities gives the best match to the observed record.

The systematic mathematical investigation of the different period multiplied phases and the features of chaos in the current model points beyond the scope of the present paper and will be reported elsewhere. Instead, we focus on the climatic relevance of the possible nonlinear responses.

5 Possible mechanism for the middle Pleistocene transition

The paleoclimatic record contains enough enigmas to realize that the Milankovitch theory of orbitally forced ice age cycles still has missing links. Especially explaining the MPT is a challenge. The 100 kyr time-scale is very long in comparison to reasonable estimates for internal climate oscillators to be at play. In Saedeleer et al. (2013), which partly inspired this work, it is proposed, based on a study of the Van de Pol oscillator, that the climatic response to orbital forcing is a phase locking of internal periods to periods of the orbital forcing. If this is the case the determining periods of the multi-period orbital forcing could potentially be identified. Here we demonstrate a different scenario for the dynamical response: First and foremost, our model does not have any internal periods of oscillation. This is a simple consequence of the fact that the proposed "climate potential" is not harmonic, thus the frequency of oscillation depends continuously on the amplitude of oscillation. The system can thus resonate with the external forcing by adjusting the amplitude of the oscillation. Furthermore, as it was seen in the case of a simple harmonic forcing, by a slow change of parameters the system can show both period doubling transitions to a chaotic state and other transitions

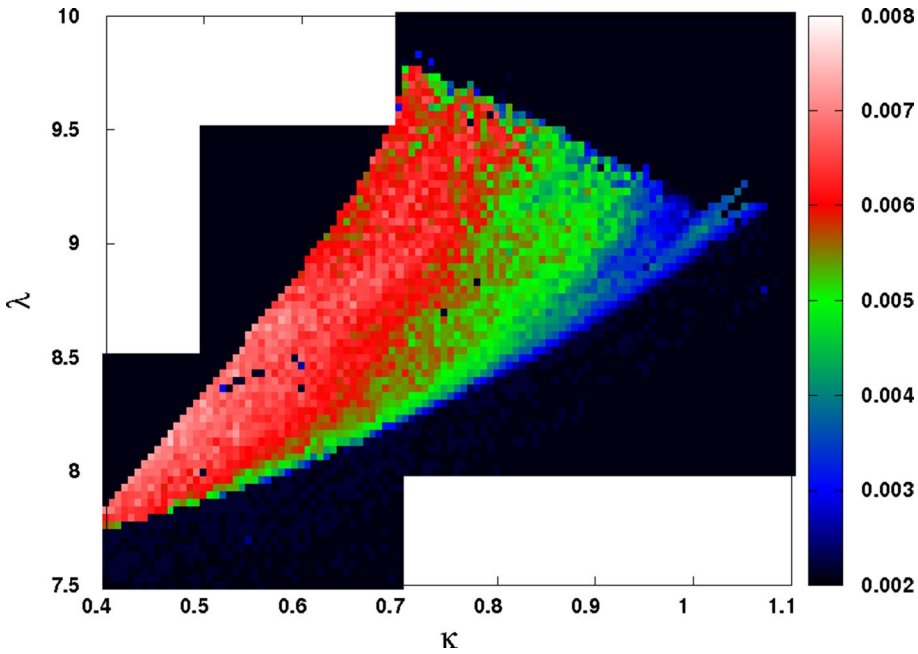

Fig. 4 Plot of the Lyapunov-exponent (in units of kyr^{-1}) for the temperature anomaly τ oscillations for a section of the (λ–κ) parameter phase space, demonstrating the presence of chaos in the model. The parameter values are $\omega = 10$, $A = 1$, and $x_0 = 0$, $\tau_0 = 1$ were used as initial conditions

such as transition to period three response. We thus propose that throughout the Pleistocene epoch, a gradual change in the climate system, which is represented by a slow variation in the model parameters, took place. Such a change is reasonable to assume as there is a long term decreasing trend in the global temperature of the Earth in the past 50 Myr (with the exception of some isolated abrupt changes induced by extreme events related to volcanos, or sharp tectonic changes). The long term global cooling can possibly be attributed to the gradual decrease of the global pCO_2 levels (Clark et al. 2006) or a possible increased stability of larger North American ice caps due to long term erosion of sediments and a subsequent decrease in sliding on the bedrock (Clark and Pollard 1998). We may assume that the relevant driving is the 41 kyr obliquity cycle throughout the Pleistocene epoch (Huybers and Wunsch 2005; Huybers 2009): In the latter part slowly varying parameters changed the dynamical response to periods two or three, thus the last part of the Pleistocene climate is interpreted as a mixture of 80 and 120 kyr responses to the obliquity cycle.

To illustrate this scenario we incorporate the assumed long-term change in the Earth's climatic response into the model by introducing a slow, gradual decrease of the climatic damping coefficient κ. In particular, we used the following form of the damping:

$$\kappa(t) = \kappa_1 + 0.5(\kappa_0 - \kappa_1)\Big\{1.0 - \tanh((t - t_0)/t_s)\Big\}, \qquad (4)$$

where $\kappa_0 > \kappa_1$, t_0, and t_s are positive constants.

Firstly, we ran the model with the real obliquity data (Berger and Loutre 1991), using $A(t) = 4(O(t) - O_{av})$, where $O(t)$ is the actual obliquity dataset and O_{av} is its time average. Figure 1 shows a MPT that was simulated using model parameters $\kappa_0 = 1.1$, $\kappa_1 = 0.3$, $t_0 = 3.5\,\text{Myr}$, $t_s = 2\,\text{Myr}$, $\lambda = 10$, and $x_0 = -1.2756$, $\tau_0 = 0$ were used as initial conditions. One can see that the period of the oscillations changed from 41 kyr to approximately 120 kyr after the MPT.

As seen in Fig. 1, the fit of the model to the climate curve is fair, but not perfect. As mentioned above, there have been quite a few different conceptual models proposed for the glacial dynamics. Some of these fit the record even better than this model does. The multitude of models implies that fitting the climate curve itself does not contain enough information to discriminate, and the apparent ease at which the climate curve can be reproduced could potentially lead to over-fitting. In case the glacial dynamics is not an entirely deterministic response to the forcing, either through critical dependence on initial conditions, chaos in the dynamics or dominance of stochastic components, a perfect model fit should not necessarily be the target. As illustration, let us imagine that the climate is driven by a purely stochastic red-noise process. If the observed record

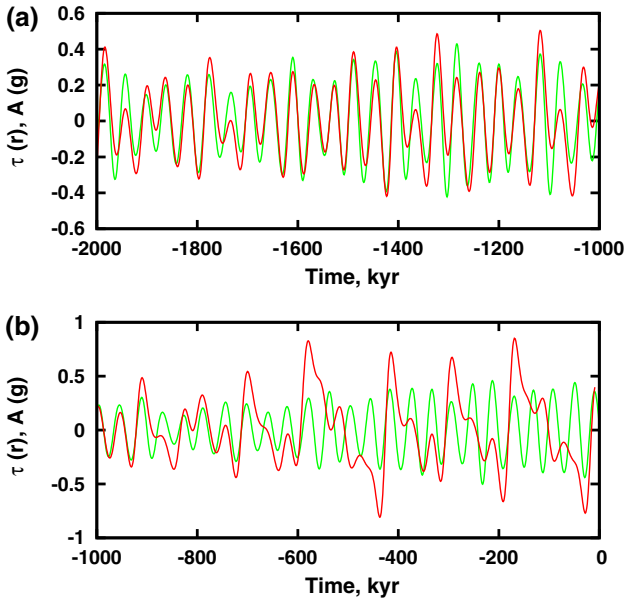

Fig. 5 The model temperature anomaly τ (*red curve*) together with the obliquity forcing A (*green curve*). Note the time; the figure has been split into to panels for clarity. The temperature oscillations lag the external drive. The *plot* shows the temperature oscillations shifted by 9 kyrs to match the phase of the obliquity oscillations. The 9 kyr lag persists through the whole model-MPT process. The parameter values used for this plot are identical with that of Fig. 1

is one realization (which we obviously cannot re-run) of the non-deterministic process, it is very difficult to assess in a meaningful way the likelihood of this one realization. The actual record can obviously be an (improbable) realization of such a proposed process. The chance that one would get exactly this realization in a model simulation is entropically prohibited. Thus the model target can only be the record in some statistical sense. Here we are guided by the connection between the climate curve and the Milankovitch forcing, and especially by the structural change at the MPT. At the level of conceptual models we have to justify that the dynamical mechanism is robust, and if there is not a perfect fit to the climate record, we argue that the observed record could be caused by the proposed dynamical mechanism.

As an additional note on the goodness of fit for the model, we observe that the maximum for the variable τ lagged 9 kyr to the maximum amplitude of the external drive, throughout the whole Pleistocene epoch. A blowup of the result is shown in Fig. 5. This result is in a good agreement with the findings in Huybers (2009).

Our proposed mechanism for changing the frequency at the MPT is rather robust with respect to the specific forcing function. Assuming the melt of the ice sheets depending on a number of degree days, we will use the summer-integrated insolation curve proposed by Huybers (2006). Depending on the length of seasonal integration the insolation curve

changes. In the one extreme of a full annual integration, where Keplers second law of the planetary orbit implies that the effect of the precessional cycles vanish and the obliquity forcing is obtained. In the other extreme of one day integration (summer solstice), the 65 summer solstice insolation curve is obtained. In between these two extremes we have also used the Huybers insolation curve, defining summer as days with insolation exceeding 275 W/m^2. The model responses for these three implemented insolation drives are shown in Fig. 6. It is clearly demonstrated that the MPT occurs in all three cases. In case of the 65N summer solstice insolation (the traditional Milankovitch curve) it is seen that prior to the MPT the model has oscillations around 20 kyr caused by the precessional cycle, in contrast to the observed 41 kyr oscillations.

Beside the change in response at the MPT the model also shows the characteristic saw-tooth shape of the oscillations after the MPT. The saw-tooth shape is a typical signature of fast-slow dynamics. To further explore this, Fig. 7 shows the details in the period three response to a sinusoidal forcing, repeating the third panel in Fig. 2. In Fig. 7a the variables $\tau(t)$ (blue), $x(t)$ (green) and the forcing $A\sin(\omega t)$ (red) are shown. The grey bands indicate the rapid warmings (fast phase), while the broad white sections indicate the gradual cooling periods (slow phase). It is important to notice that the forcing (red curve) differs strongly for the two fast phase periods, while $x(t)$ is almost identical for the two periods.

The multiplicative coupling term $xA\sin(\omega t)$ is shown in Fig. 7b, red curve. The model illustrates that glacial terminations do not have to be in phase with the change in orbital forcing. The fast transitions are solely caused by the "potential drift" term $-dV/dx$, which is shown in Fig. 7b, blue curve. To illustrate this further, a phase space portrait of the period three cycle is shown in Fig. 7c while the trajectory of the forcing versus x is shown in Fig. 7d. The coloring of the curves is such that the red part corresponds to the fast phases and the blue part to the slow phases. The fast-slow dynamics is thus a consequence of the asymmetry in the internal dynamics, represented in the simple model by the skewed climate potential, shown in Fig. 7e. Again, the red part corresponds to the fast periods while the blue part corresponds to the slow periods. The obvious candidate for a physical explanation of the asymmetry is that the melting and collapse of ice sheets and perhaps the melting of sea ice is a much faster process than the buildup of ice sheets from precipitation.

The glacial oscillations after the MPT are apparently much less regular than the 41 kyr period oscillations prior to the MPT. This could indicate either that the latter oscillations are such that they vary between a regime of period two and a regime of period three response or the response is simply a long transient response before the system settles

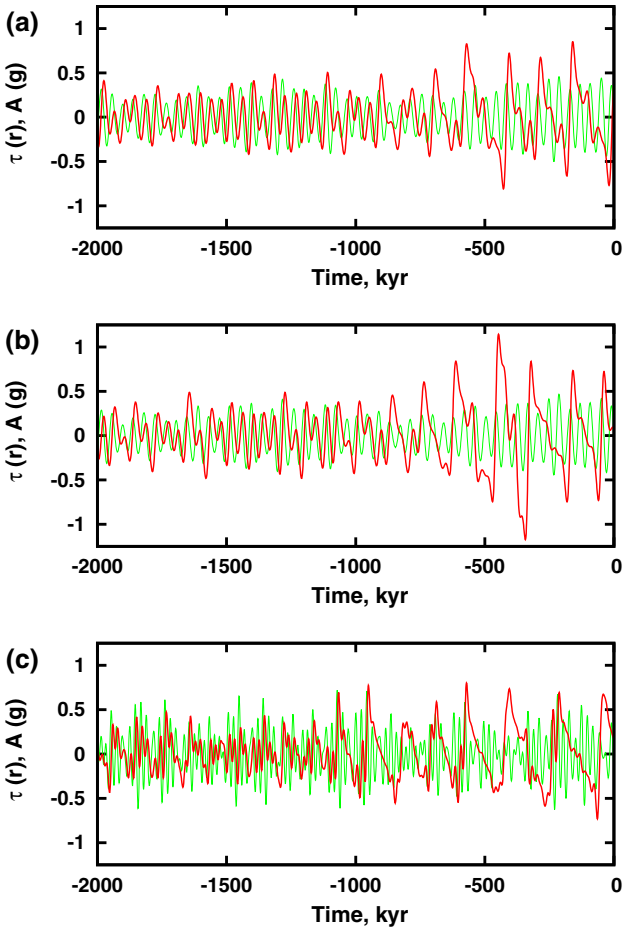

Fig. 6 Model temperature anomaly τ response to different climatic drives A. **a** Obliquity forcing (Berger and Loutre 1991) (with parameters $A = 4$, $\kappa_0 = 1.1$, $\kappa_1 = 0.3$, $t_0 = 3.5$ Myr, $t_s = 2.008$ Myr), **b** Huybers integrated insolation forcing (Huybers 2006) (with parameters $A = 40$, $\kappa_0 = 2.3$, $\kappa_1 = 0.1857$, $t_0 = 2$ Myr, $t_s = 2$ Myr), and **c** 65N summer solstice insolation drive (Berger 1978) (with parameters $A = 0.12$, $\kappa_0 = 2.1$, $\kappa_1 = 0.3$, $t_0 = 2$ Myr, $t_s = 2$ Myr). The red curves correspond to the temperature anomaly (τ), while the green curves represent the respective climatic drives (average substracted and multiplied by the respective model amplitude A). One can see the robustness of the model response: The presence of MPT and the features of the post-MPT saw-tooth climatic oscillations are not sensitive to the particular type of implemented climatic forcing. The other parameter values are $\lambda = 10$, $\alpha = 0.8$, and $x_0 = -1.2756$, $\tau_0 = 0$ were used as initial conditions

into a period three regime. This points to the fundamental issue of climate predictability, since the model shows both critical dependence on initial conditions and chaotic regimes. These are not synonymous, since the first can arise due to non-trivial boundaries for basins of attraction of different solutions even in the non-chaotic regime. To illustrate this, we made a small perturbation on the slow temporal change of the climatic damping coefficient. We found that even such a small disturbance gets amplified and shifts a glacial by a whole obliquity cycle (41 kyr) after 0.5 Myr

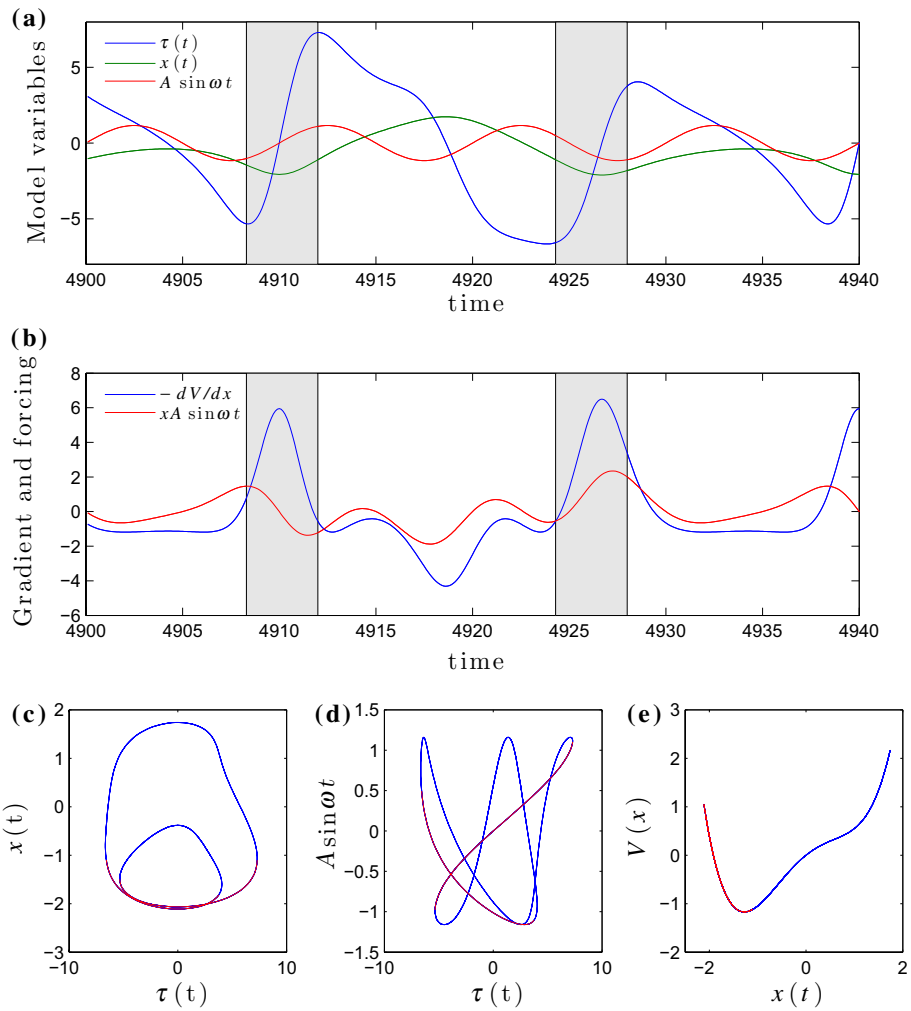

Fig. 7 The period three response to a sinusoidal forcing, as in Fig. 2. The parameter values are $\alpha = 0.8, \lambda = 0.087, \kappa = 0.078$, $A = 1.16, \omega = 2\pi/10$. **a** The variables τ (*blue*), $x(t)$ (*green*) and $A\sin(\omega t)$ (*red*). The *grey bands* with rapid increase in τ are defined as the fast periods, while the rest are the slow periods. **b** The two dominant terms in the *right hand side* of the dynamical Eq. (2): $-dV/dx$ (*blue*) and $xA\sin(\omega t)$ (*red*). It is seen that the fast dynamics is governed by the former term, representing internal dynamics. **c** The phase space portrait of the period three solution, while **d** shows the forcing $A\sin(\omega t)$ versus τ. **e** The "climate potential". The asymmetry of the potential is responsible for the fast-slow dynamics and the saw-tooth shape of the record. The *red parts of the curves* in **c**–**e** correspond to the fast periods

later, constituting a critical dependence on parameters. For this range of parameters, there is no chaos in the system when it is driven by a simple sinusoidal oscillation. As seen from the existence of positive Lyapunov exponents (Fig. 4) for some parameter values (in the case of a simple sinusoidal forcing) shows that critical dependence on initial conditions also exists in this case. For the system to be chaotic in the mathematical sense it also has to be topologically mixing (any open set in attractor will evolve to cover the attractor densely) and there exists a series of periodic orbits which will converge to any trajectory on the attractor. The question of if and under which conditions true chaos exists in the model is beyond our scope here.

6 Summary

We have formulated a conceptual model to describe the MPT as a shift from a period one to a period two and period three response to the 41 kyr obliquity forcing of the Milankovitch theory: The eccentricity cycle is omitted all together in the forcing, and the late Pleistocene 100 kyr world is still reproduced. The change at the MPT is caused by a long term, gradual decrease of some parameter of the system. With this conceptual model approach, we can only point to dynamical mechanisms and not to the real environmental change. However, the idea of a gradual change aligns with the decrease in global $p\mathrm{CO}_2$ or tectonic rearrangements as proposed in the literature.

The model does not in itself possess an internal frequency of oscillation, thus suggesting that the time-scale of the glacial cycles is determined solely by the non-linear response to the frequency of the obliquity pacing. We observe that the model reproduces the observed saw-tooth shaped time reversal asymmetry observed in the record, which is not present in the forcing. In the model this is related to the larger amplitude of the glacial cycles after the MPT in comparison to the more symmetric cycles prior to the MPT. With the larger cycles, the system experiences the non-linearity in the internal dynamical response (the climate potential in the model) much stronger than in the case of small, almost harmonic oscillations. As we have shown,

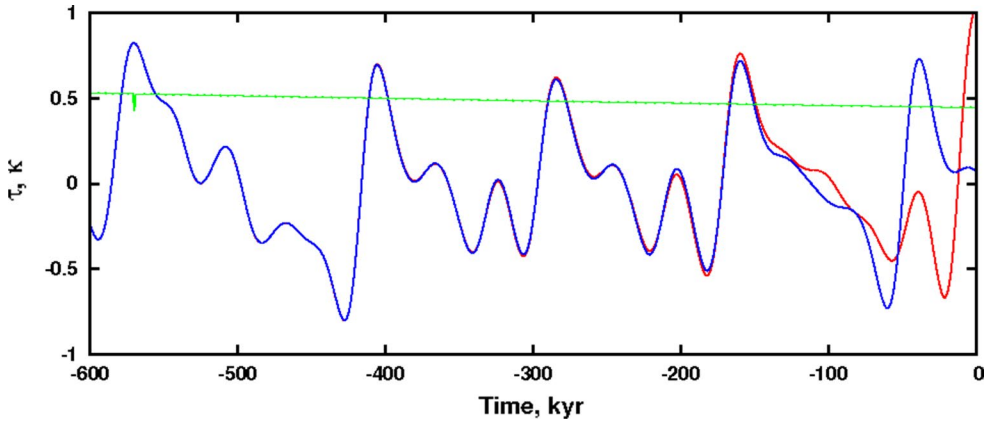

Fig. 8 A small perturbation in the climatic damping coefficient (*green curve*) leads to a remarkable shift of the glacial cycles, constituting a climatic butterfly effect. The *blue* and *red* curves correspond to the resulting temperature anomalies τ without and with the perturbation in the slowly decreasing climatic damping coefficient, both driven by real obliquity data (Berger 1978), in the same way as described in the text for Fig. 1. The parameter values are $\lambda = 10$, $\kappa_0 = 1.1$, $\kappa_1 = 0.3$, $t_0 = 3.5\,\text{Myr}$, $t_s = 2.008\,\text{Myr}$, and $x_0 = -1.2756$, $\tau_0 = 0$ were used as initial conditions

the modulations in the forcing amplitude can also lead to a change in the periodicity of the response.

Despite its simplicity, the model shows a surprisingly wide range of behaviours depending on the forcing, the initial conditions and the values of the parameters. The observed variety of possible climatic responses in the model raises the perplexing question: How robust is the climatic history of the Earth? We are obviously not in the position where we can rerun the past. Thus we must ask in which sense, we should be able to model the past, by reproducing the evolution, which has been realised, or by reproducing the past in some statistical sense.

Furthermore, the presence of critical dependence on initial conditions in the present model suggests that this could be manifested in the climate system itself in a so-called climatic butterfly effect: A small perturbation, or even just the internal climatic noise, might cause a significant shift in the glacial cycles (Fig. 8). Obviously, this could impose fundamental limitations on long-term climate predictability.

Acknowledgments I. D. acknowledges the support of the Hungarian Science Foundation under the contract OTKA NK72037 and that of the Hungarian Meteorological Service. We thank Michel Crucifix and one anonymous reviewer for constructive comments.

References

Ashkenazy Y, Tziperman E (2004) Are the 41 kyr oscillations a linear response to Milankovitch forcing? Quat Sci Rev 23:1879–1890

Augustin L, Barbante C, Barnes PR et al (2004) Eight glacial cycles from an Antarctic ice core. Nature 429:623–628

Benzi R, Parisi G, Sutera A, Vulpiani A (1982) Stochastic resonance in climatic change. Tellus 34:10–16

Berger AL (1978) Long-term variations of daily insolation and quaternary climatic changes. J Atmos Sci 35:2362–2367

Berger A (1988) Milankovitch theory and climate. Rev Geophys 26:624–657

Berger A (2012) A brief history of the astronomical theories of paleoclimates. In: Berger A et al (eds) Climate change. Springer, Wien, pp 107–129

Berger A, Loutre MF (1991) Insolation values for the climate of the last 10 million of years. Quat Sci Rev 10:297–317

Budyko MI (1969) The effect of solar radiation changes on the climate of the Earth. Tellus 21:611–619

Chekroun MD, Simonnet E, Ghil M (2011) Stochastic climate dynamics: random attractors and time-dependent invariant measures. Phys D 240(21):1685–1700

Clark PU, Archer D, Pollard D, Blum JD, Rial JA, Brovkin V, Mix AC, Pisias NG, Roy M (2006) The middle Pleistocene transition: characteristics, mechanisms, and implications for long-term changes in athmospheric pCO_2. Quat Sci Rev 25:3150–3184

Clark PU, Pollard D (1998) Origin of the middle Pleistocene transition by ice sheet erosion of regolith. Paleoceanography 13:1–9

Crucifix M (2012) Oscillators and relaxation phenomena in Pleistocene climate theory. Philos Trans R Soc A 370:1140–1165

Crucifix M (2013) Why could ice ages be unpredictable? Clim Past 9:2253–2267

De Saedeleer B, Crucifix M, Wieczorek S (2013) Is the astronomical forcing a reliable and unique pacemaker for climate? A conceptual model study. Clim Dyn 40:273–294

Ditlevsen PD (2009) Bifurcation structure and noise-assisted transitions in the Pleistocene glacial cycles. Paleoceanography 24:PA3204

Hays JD, Imbrie J, Shackleton NJ (1976) Variations in the Earth's orbit: pacemaker of the ice ages. Science 194:1121–1132

Hoffman PF, Kaufman AJ, Halverson GP, Schrag DP (1998) A Neoproterozoic snowball Earth. Science 281:1342–1346

Huybers P (2006) Early Pleistocene glacial cycles and the integrated summer insolation forcing. Science 313:508–511

Huybers P (2007) Glacial variability over the last two million years: an extended depth-derived age model, continuous obliquity pacing, and the Pleistocene progression. Quat Sci Rev 26:37–55

Huybers P (2009) Pleistocene glacial variability as a chaotic response to obliquity forcing. Clim Past 5:481–488

Huybers P, Wunsch C (2005) Obliquity pacing of the late Pleistocene glacial terminations. Nature 434:491–494

Hyde WT, Peltier WR (1985) Sensitivity experiments with a model of the ice age cycle: the response to harmonic forcing. J Atmos Sci 42:2170–2188

Imbrie J, Berger A, Boyle EA, Clemens SC, Duffy A, Howard WR, Kukla G, Kutzbach J, Martinson DG, McIntyre A, Mix AC, Molfino B, Morley JJ, Peterson LC, Pisias NG, Prell WL, Raymo ME, Shackleton NJ, Toggweiler JR (1993) On the structure and origin of major glaciation cycles 2. The 100,000-year cycle. Paleoceanography 8:699–735

Imbrie JZ, Imbrie-Moore A, Lisiecki LE (2011) A phase-space model for Pleistocene ice volume. Earth Planet Sci Lett 307(94):102

Kallen E, Crafoord C, Ghil M (1979) Free oscillations in a climate model with ice-sheet dynamics. J Atmos Sci 36:2292–2303

LeTreut H, Ghil M (1983) Orbital forcing, climate interactions, and glacial cycles. J Geophys Res 88:5167–5190

Lisiecki LE, Raymo ME (2005) A Pliocene–Pleistocene stack of 57 globally distributed benthic D18O records. Paleoceanography 20:PA1003

Paillard D (1998) The timing of Pleistocene glaciations from a simple multiple-state climate model. Nature 391:378–381

Paillard D, Parrenin F (2004) The Antarctic ice sheet and the triggering of deglaciations. Earth Planet Sci Lett 227:263–271

Petit JR et al (2001) Vostok ice core data for 420,000 years, IGBP PAGES/World Data Center for Paleoclimatology data contribution series no. 2001–076. NOAA/NGDC Paleoclimatology Program, Boulder CO, USA

Rial JA (2004) Abrupt climate change: chaos and order at orbital and millennial scales. Glob Planet Change 41:95–109

Saltzman B, Maasch K (1991) A first-order global model of late Cenozoic climate change II: a simplification of CO_2 dynamics. Clim Dyn 5:201–210

Sellers WD (1969) A climate model based on the energy balance of the earth–athmosphere system. J Appl Meteorol 8:392–400

Shackleton NJ (1997) Deep-sea sediment record and the Pliocene–Pleistocene boundary. Quart Int 40:33–35

Tziperman E, Gildor H (2003) On the mid-Pleistocene transition to 100-kyr glacial cycles and the asymmetry between glaciation and deglaciation times. Paleoceanography 18:1–8

Tziperman E, Raymo ME, Huybers P, Wunsch C (2006) Consequences of pacing the Pleistocene 100 kyr ice ages by nonlinear phase locking to Milankovitch forcing. Paleoceanography 21:PA4206